



ECAP process improvement based on the design of rational inclined punch shapes for the acute-angled Segal 2θ -dies: CFD 2-D description of dead zone reduction

A. V. Perig¹ and N. N. Golodenko²

¹Manufacturing Processes and Automation Engineering Department, Donbass State Engineering Academy, Shkadinova Str. 72, 84313 Kramatorsk, Ukraine

²Department of Water Supply, Water Disposal and Water Resources Protection, Donbass National Academy of Civil Engineering and Architecture, Derzhavin Str. 2, 86123 Makeyevka, Ukraine

Correspondence to: A. V. Perig (olexander.perig@gmail.com)

Received: 27 July 2014 – Revised: 22 March 2015 – Accepted: 5 April 2015 – Published: 14 April 2015

Abstract. This article is focused on a 2-D fluid dynamics description of punch shape geometry improvement for Equal Channel Angular Extrusion (ECAE) or Equal Channel Angular Pressing (ECAP) of viscous incompressible continuum through acute-angled Segal 2θ -dies with $2\theta < 90^\circ$. It has been shown both experimentally with physical simulation and theoretically with computational fluid dynamics that for the best efficiency under the stated conditions, the geometric condition required is for the taper angle $2\theta_0$ of the inclined oblique punch to be equal to the 2θ angle between the inlet and outlet channels of the Segal 2θ -die. Experimentally and theoretically determined rational geometric condition for the ECAP punch shape is especially prominent and significant for ECAP through the acute angled Segal 2θ -dies. With the application of Navier-Stokes equations in curl transfer form it has been shown that for the stated conditions, the introduction of an oblique inclined $2\theta_0$ -punch results in dead zone area downsizing and macroscopic rotation reduction during ECAP of a viscous incompressible continuum. The derived results can be significant when applied to the improvement of ECAP processing of both metal and polymer materials through Segal 2θ -dies.

1 Introduction

For the last 20 years a number of research efforts in materials science related fields have been focused on wider development, implementation, commercialization and improvement of new material forming methods known as Severe Plastic Deformation (SPD) schemes (Boulaia et al., 2009; Haghighi et al., 2012; Han et al., 2008; Laptev et al., 2014; Minakowski, 2014; Nagasekhar et al., 2006; Nejadseyfi et al., 2015; Perig et al., 2013a, b, 2015; Perig and Laptev, 2014; Perig, 2014; Rejaeian and Aghaie-Khafri, 2014). The classical SPD processing method is Segal's Equal Channel Angular Extrusion (ECAE) or Equal Channel Angular Pressing (ECAP) material forming technique (Segal, 2004). ECAE or ECAP realization is based on one or several extrusion

passes of a lubricated metal or polymer material through a die with two intersecting channels of equal cross-section (Segal, 2004). Materials' processing by ECAP results in the accumulation of large shear strains and material structure refinement with physical properties enhancement (Boulaia et al., 2009; Nagasekhar et al., 2006; Nejadseyfi et al., 2015; Segal, 2004). The standard die geometry ABC-abc for ECAP processing is the so-called Segal 2θ -die geometry, where the inlet AB-ab and outlet BC-bc die channels have an intersection angle 2θ (Figs. 1–2). Moreover Segal 2θ -dies have neither external nor internal radii at the channel intersection points B; b (Figs. 1–2).

In recent years we have seen major research interest in the introduction of fluid mechanics techniques (Minakowski, 2014; Perig et al., 2010; Perig and Golodenko, 2014a, b; Re-

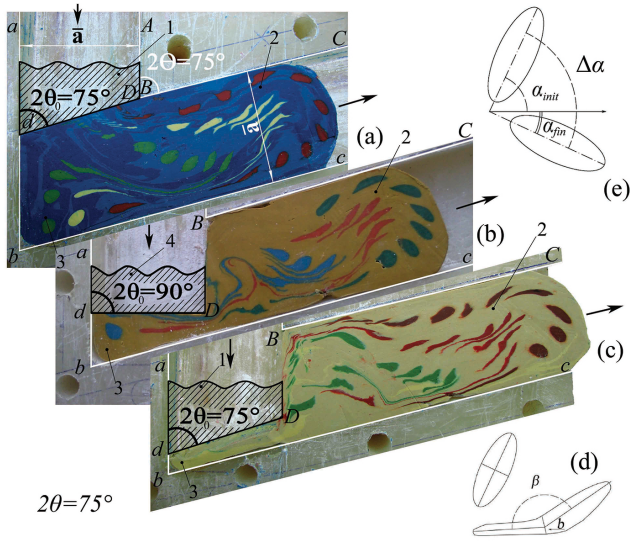


Figure 1. Physical simulation with soft model-based experiments of punch shape (1, 4) influence on ECAP flow of viscous continuum (2) through acute-angled Segal die ABC-abc with channel intersection angle $2\theta = 75^\circ < 90^\circ$: (4) classical punch of rectangular shape dD in (b); (1) modified shape of inclined $2\theta_0$ -punch dD in (a) and (c), where $2\theta_0 = 2\theta$; (3) the experimentally derived shape of the dead zone for material flow during ECAP; the schematic diagrams of macroscopic rotation (e) and rotational inhomogeneity (d) formation during viscous continuum ECAP.

jaeian and Aghaie-Khafri, 2014) to the solution of ECAP problems. This interest is results from growing application of ECAP SPD techniques to processing of polymers (Boulahia et al., 2009; Perig et al., 2010; Perig and Golodenko, 2014a, b) and powder materials (Haghighi et al., 2012; Nagasekhar et al., 2006) where viscosity effects become essential.

At the same time the phenomenological description of polymer materials flow through Segal 2θ -dies with Navier-Stokes equations has not been adequately addressed in previously known publications (Minakowski, 2014; Perig et al., 2010; Perig and Golodenko, 2014a, b; Rejaeian and Aghaie-Khafri, 2014). This underlines the importance of the present research, dealing with fluid dynamics 2-D simulation of material flow through the acute-angled Segal 2θ -dies with channel intersection angles of $2\theta > 0^\circ$ and $2\theta < 90^\circ$.

Another problem during ECAP material processing through the acute-angled Segal 2θ -dies with $2\theta < 90^\circ$ is connected with the formation of large dead zones (3) in the viscous material flow in Fig. 1b as well as enormous and dangerous mixing $\Delta\alpha$ of viscous material (2) in Fig. 1b and e during viscous continuum ECAP through acute-angled dies with channel intersection angles of $2\theta < 90^\circ$ when standard classical rectangular punches (4) are applied (Fig. 1b). So simple physical simulation experiments in Fig. 1b for viscous continuum ECAP through the die ABC-abc with $2\theta = 75^\circ$ confirm the disadvantages of using a standard punch (4) with

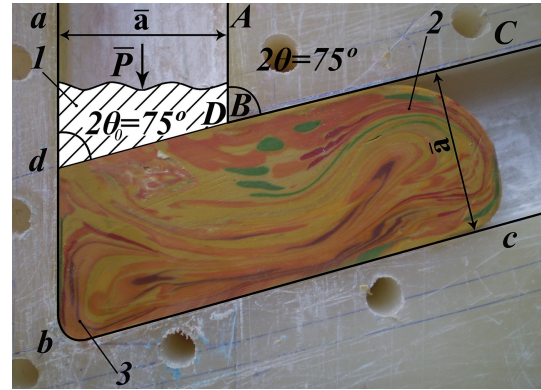


Figure 2. Soft physical model of the workpiece after 3 ECAP passes through Segal 2θ -die via route C with modified shape of $2\theta_0$ -inclined or $2\theta_0$ -beveled punch, where $2\theta = 2\theta_0 = 75^\circ$.

rectangular shape AD-ad ($2\theta_0 = 90^\circ$) in Fig. 1b. It is very important to note that known approaches in published articles (Boulahia et al., 2009; Haghighi et al., 2012; Han et al., 2008; Laptev et al., 2014; Minakowski, 2014; Nagasekhar et al., 2006; Nejadseyfi et al., 2015; Perig et al., 2013a, b; Perig and Laptev, 2014; Perig, 2014; Rejaeian and Aghaie-Khafri, 2014; Segal, 2004; Wu and Baker, 1997) have never addressed the possibility of changing the standard rectangular punch shape AD-ad in Fig. 1b for material ECAP through acute-angled Segal dies with $2\theta < 90^\circ$.

This fact emphasizes the importance and underlines the prime novelty of the present article addressing the viscous fluid dynamics description of the influence of classical (Fig. 1b) and novel modified $2\theta_0$ -inclined or $2\theta_0$ -beveled (Figs. 1a, c and 2) punch shape AD-ad on viscous flow features of processed workpieces during ECAP SPD pressure forming through acute-angled Segal 2θ -dies with channel intersection angles of $2\theta > 0^\circ$ and $2\theta < 90^\circ$.

2 Aims and scopes of the article – prime novelty statement of research

The present article is focused on the experimental and theoretical description of viscous workpiece flow through 2θ acute-angled angular dies of Segal geometry during ECAP by a classical rectangular punch and a novel modified $2\theta_0$ -inclined or $2\theta_0$ -beveled punch.

The aim of the present research is the phenomenological continuum mechanics based description of viscous workpiece flow through the 2θ acute-angled angular dies of Segal geometry during ECAE with an application of classical rectangular and novel modified $2\theta_0$ -inclined or $2\theta_0$ -beveled punch shapes.

The subject of the present research is the process of ECAP working through the 2θ acute-angled angular dies of Segal geometry with viscous flow of polymeric workpiece mod-

els, forced by the external action of classical rectangular and novel modified $2\theta_0$ -inclined or $2\theta_0$ -beveled punch shapes.

The object of the present research is to establish the characteristics of the viscous flow of workpiece models through the 2θ acute-angled angular dies of Segal geometry with respect to workpiece material rheology and geometric parameters of different punch shapes on viscous ECAP process.

The experimental novelty of the present article is based on the introduction of initial circular gridlines to study the punch shape influence on viscous workpiece ECAP flow through the 2θ angular acute-angled dies of Segal geometry.

The prime novelty of the present research is the numerical finite-difference solution of Navier-Stokes equations in the curl transfer form for the viscous workpiece flow through 2θ acute-angled angular dies of Segal geometry during ECAP, taking into account the classical rectangular and novel modified $2\theta_0$ -inclined or $2\theta_0$ -beveled punch shapes.

3 Physical simulation study of punch shape influence on viscous flow

Physical simulation techniques using plasticine workpiece models are often used in material forming practice (Chijiwa et al., 1981; Han et al., 2008; Laptev et al., 2014; Perig et al., 2010, 2013a, b, 2015; Perig and Laptev, 2014; Perig and Golodenko, 2014a, b; Perig, 2014; Sofuoglu and Rasty, 2000; Wu and Baker, 1997).

In order to estimate the character of viscous flow during ECAP through a 2θ acute-angled angular die of Segal geometry ABC-abc under the action of a classical rectangular punch and a novel modified $2\theta_0$ -inclined or $2\theta_0$ -beveled punch shapes we have utilized physical simulation techniques in Figs. 1–2. The plasticine workpiece models in Figs. 1–2 have been extruded through a ECAP die ABC-abc with channel intersection angle $2\theta = 75^\circ$ using a standard punch (4) with rectangular shape ($2\theta_0 = 90^\circ$) in Fig. 1b and novel modified $2\theta_0 = 75^\circ$ -inclined or $2\theta_0 = 75^\circ$ -beveled punch (1) in Figs. 1a, c and 2 as the first experimental approach to polymeric materials flow (Figs. 1–2).

The aim of the physical simulation is an experimental study of dead zone abc formation and deformation zone abc location during viscous ECAP flow of workpiece plasticine models under the external action of rectangular and inclined punches. The physical simulation in Figs. 1–2 is also focused on the experimental visualization of rotary modes of SPD during ECAP of viscous polymer models for the different punch geometries. The experimental results in Figs. 1–2 are original experimental research results, obtained by the authors.

The plastic die model of ECAP die ABC-abc with channel intersection angle $\angle ABC = \angle abc = 2\theta = 75^\circ$ and the width of inlet aA and outlet cC die channels 35 mm is shown in Figs. 1–2. Potato flour was used as the lubricator in Figs. 1–2.

The main experimental visualization technique in Figs. 1–2 is based on the manufacture of the initial plasticine physical models of the workpieces in the shapes of rectangular parallelepipeds, freezing of these rectangular parallelepipeds, marking the initial circular gridlines on the front sides of the frozen parallelepipeds, perforation of through-holes in the parallelepipeds at the centers of the initial circular gridlines, repeated freezing of the plasticine (Fig. 1) parallelepipeds, heating of the plasticine (Fig. 1) pieces with different colors to the half-solid state, and placing the half-solid multicolor plasticine (Fig. 1) into the through-holes of the frozen parallelepipeds using a squirt without needle technique.

In this way the initial plasticine-based (Fig. 1) circular gridlines were marked throughout the initial plasticine (Fig. 1) workpieces. The initial circular gridlines transform into deformed elliptical ones as workpieces flow from inlet to outlet die channels during ECAP (Figs. 1a, c and 2). The gridline-free dead zones (p. b) were visualized through the physical simulation techniques introduction in Figs. 1–2. It was found that dead zone (p. b) formation takes place in the vicinity of the external angle abc of channel intersection zone Bb. It was experimentally shown that the best reduction of dead zone size (3) for an ECAE die with $2\theta = 75^\circ$ could be achieved through the replacement of the standard rectangular punch AD-ad with ($2\theta_0 = 90^\circ$) in Fig. 1b with the new $2\theta_0$ -inclined or $2\theta_0$ -beveled punch AD-ad with $2\theta_0 = 75^\circ$.

It was experimentally found in Figs. 1–2 that the deformation zone BCDC during ECAP of the viscous models is not located in the channel intersection zone Bb but is located in the beginning of the outlet die channel BC-bc. The relative location of the elliptical markers in outlet die channel BC-bc show the formation of two rotary modes of SPD during ECAP (Fig. 1).

Checking the successive locations of one color elliptical markers in Fig. 1, we see that the major axis of every elliptical marker rotates with respect to the axis of the outlet die channel bc. We define the term of macroscopic rotation as the relative rotation of the major axis of an elliptical marker with respect to the flow direction axis bc. The macroscopic rotation is the first visually observable rotary mode during ECAP forming of the viscous workpiece model.

Visual comparison of Fig. 1b with Figs. 1a, c and 2 shows that the macroscopic rotation is an unknown function of ECAP die channel intersection angle 2θ and $2\theta_0$ -punch shape geometry. However under SPD ECAP treatment some deformed elliptical markers within the viscous material have additional bending points and have the form of “commas” or “tadpoles” in Figs. 1–2. If the elliptical marker has an additional bending point during ECAP, then we will call the vicinity of the marker with this “waist” as a zone of rotational inhomogeneity within the workpiece material, which is usually located at the beginning of the outlet die channel BC-bc in Figs. 1–2. The rotational inhomogeneity is the second visually observable rotary mode during ECAP forming of the viscous workpiece model, which strongly depends on

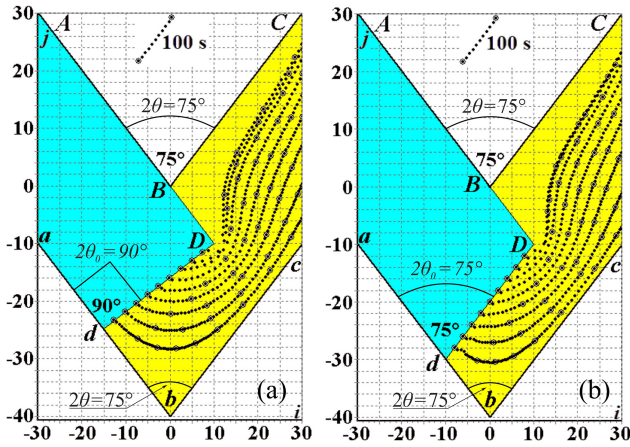


Figure 3. Computational flow lines for the Segal die with $2\theta = 75^\circ$ for the coordinate steps $\bar{\xi} = 1.10\text{ mm}$; $\bar{\eta} = 1.44\text{ mm}$ for the rectangular punch dD ($2\theta_0 = 90^\circ$) (a) and for the inclined punch dD ($2\theta_0 = 75^\circ$) (b), where time iteration step is $\bar{t}_{it} = 610\ \mu\text{s}$, transition time is $\bar{t}_{tr} = 11.3\text{ s}$.

the ECAP die channel intersection angle 2θ and $2\theta_0$ -punch shape geometry.

The experimental results in Figs. 1–2 have indicated the formation of the following zones within worked materials' volumes: (I) the dead zone (p. b); (II) the deformation zone BCDc; (III) the macroscopic rotation zone (BC-bc), and (IV) the zone of rotational inhomogeneity (BC-bc). The complex of physical simulation techniques in Figs. 1–2 introduces the initial circular gridlines technique with the application of plasticine workpieces with the initial circular colorful gridlines in the shape of initial colorful cylindrical plasticine inclusions (Fig. 1). The application of the initial circular gridlines experimental technique and the introduction of a novel modified $2\theta_0$ -inclined or $2\theta_0$ -beveled punch shapes has not been addressed in previous known ECAP research (Boulaia et al., 2009; Haghighi et al., 2012; Han et al., 2008; Laptev et al., 2014; Minakowski, 2014; Nagasekhar et al., 2006; Nejadseyfi et al., 2015; Perig et al., 2013a, b; Perig and Laptev, 2014; Perig, 2014; Rejaeian and Aghaie-Khafri, 2014; Segal, 2004; Wu and Baker, 1997).

The proposed complex of experimental techniques for physical simulation of SPD during ECAP in Figs. 1–2 will find the further applications in the study of viscous ECAP through the dies with more complex Iwahashi, Luis-Perez, Utyashev, Conform and equal radii geometries for the different punch shape geometries and different routes of multi-pass ECAP working.

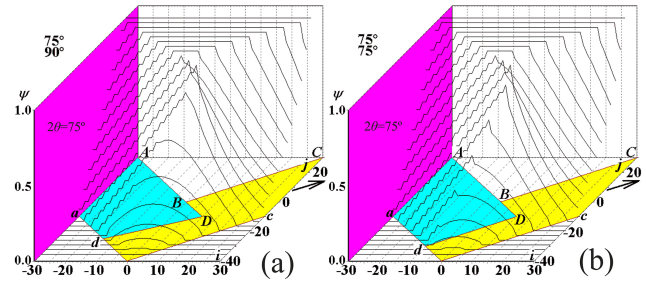


Figure 4. Computational dimensionless flow function ψ for the Segal die with $2\theta = 75^\circ$ for the rectangular punch dD ($2\theta_0 = 90^\circ$) (a) and for the inclined punch dD ($2\theta_0 = 75^\circ$) (b).

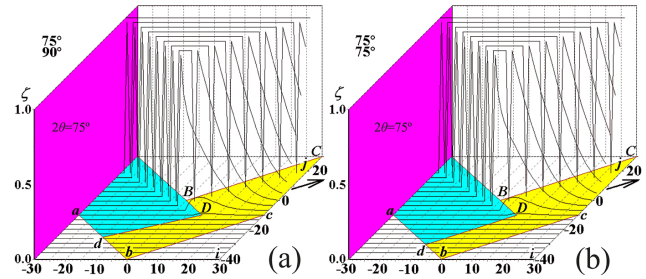


Figure 5. Computational dimensionless curl function ζ for the Segal die with $2\theta = 75^\circ$ for the rectangular punch dD ($2\theta_0 = 90^\circ$) (a) and for the inclined punch dD ($2\theta_0 = 75^\circ$) (b).

4 Numerical simulation study of punch shape influence on flow lines, and punching pressure during viscous ecap flow through Segal 2θ -dies

In order to derive the mathematical model of the viscous material flow during ECAP through the acute-angled Segal 2θ -die taking into account the punch shape AD-ad effect on viscous flow dynamics we will apply the Navier-Stokes equations (Appendices A–D). The results of the numerical simulation study are shown in computational diagrams in Figs. 3–10.

Computational results in Figs. 3–10 illustrate the punch shape influence on geometry (Fig. 3), kinematics (Figs. 4–8) and dynamics (Figs. 9–10) of the viscous flow during ECAP. Computational plots in Figs. 3–10 are based on a finite-difference solution of the Navier–Stokes equations in curl transfer form Eqs. (A1)–(A2) with initial Eq. (B1) and boundary Eqs. (C1)–(C7) conditions.

Instabilities of the numerical solutions, which appear at the outlet frontiers cC (Figs. 3–10), propagate upstream.

CFD-derived computational flow lines in Fig. 3b directly show the reduction of dead zone area dDbc when we use the modified $2\theta_0$ -inclined or $2\theta_0$ -beveled punch shape, where $2\theta = 2\theta_0 = 75^\circ$ (Fig. 3b). CFD-derived computational flow lines in Fig. 3a also outline the largest dead zone area dDbc when we use the standard punch (Fig. 3a) with rectangular shape ($2\theta_0 = 90^\circ$). CFD-derived computational di-

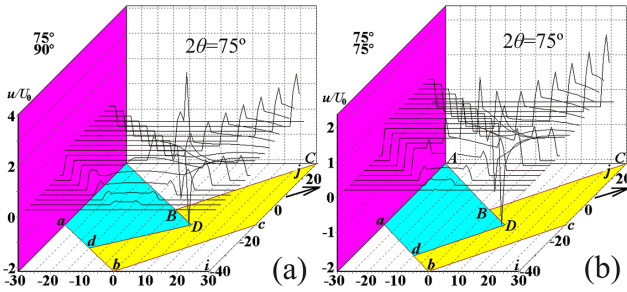


Figure 6. Computational u components of flow velocities for the Segal die with $2\theta = 75^\circ$ for the rectangular punch dD ($2\theta_0 = 90^\circ$) (a) and for the inclined punch dD ($2\theta_0 = 75^\circ$) (b).

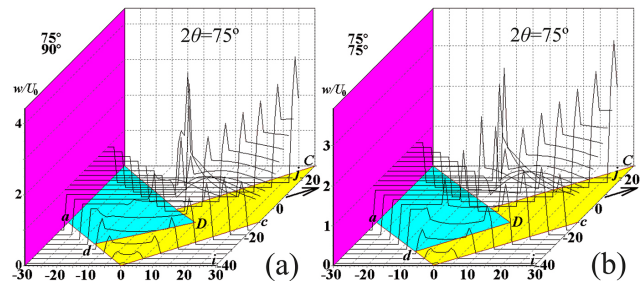


Figure 8. Computational dimensionless full flow velocities w for the Segal die with $2\theta = 75^\circ$ for the rectangular punch dD ($2\theta_0 = 90^\circ$) (a) and for the inclined punch dD ($2\theta_0 = 75^\circ$) (b).

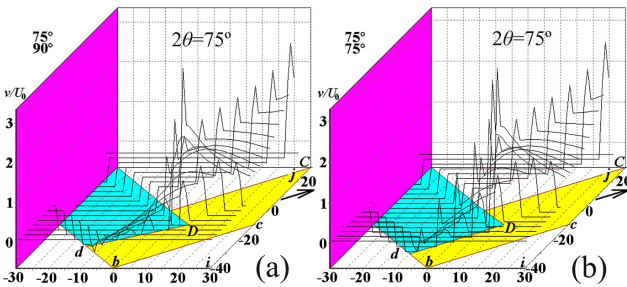


Figure 7. Computational v components of flow velocities for the Segal die with $2\theta = 75^\circ$ for the rectangular punch dD ($2\theta_0 = 90^\circ$) (a) and for the inclined punch dD ($2\theta_0 = 75^\circ$) (b).

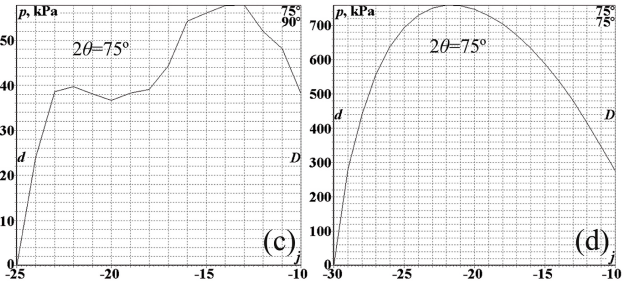
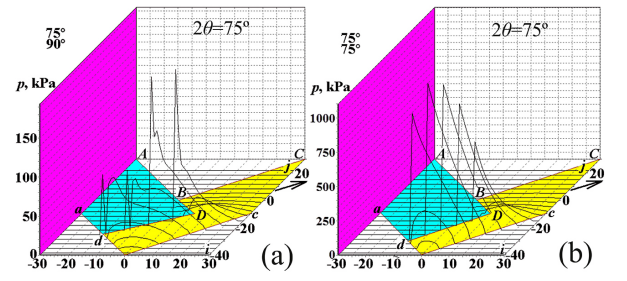


Figure 9. Computational dimensionless punching pressure for the Segal die with $2\theta = 75^\circ$ for the rectangular punch dD ($2\theta_0 = 90^\circ$) (a, c) and for the inclined punch dD ($2\theta_0 = 75^\circ$) (b, d).

agrams for ECAP punching pressure in Figs. 9–10 show that the application of the standard rectangular punch with $2\theta_0 = 90^\circ$ requires lower punching pressures (Fig. 10). The CFD-based simulation in Figs. 9–10 indicates that the use of the modified $2\theta_0$ -inclined or $2\theta_0$ -beveled punch shapes requires higher punching pressures for ECAP of viscous incompressible continuum through the acute-angled Segal 2θ -dies with $2\theta < 90^\circ$.

Higher values of punching pressure for modified $2\theta_0$ -inclined or $2\theta_0$ -beveled punch shapes in comparison with the standard rectangular punch with $2\theta_0 = 90^\circ$ in Figs. 9–10 result from the fact that the compressive strains in such schemes are higher than shear strains.

So in order to force the plasticine model through the 2θ -die by the modified $2\theta_0$ -inclined punch we have to apply higher punching force in order to reach the necessary shear stresses. This fact is shown in Figs. 9–10.

The increased punching pressure required for the modified $2\theta_0$ -inclined punches and for the acute angled 2θ -dies with $2\theta < 90^\circ$ results in decreased dead zone in angle b and a decreased shear stress component (Figs. 6b, 7b, 8b, 9b, d, and 10).

For the modified $2\theta_0$ -inclined punches and the obtuse angled 2θ -dies with $2\theta > 90^\circ$ the decreased punching pressure results from increased effective punch area dD and increased shear stress component (Fig. 10).

5 Discussion of derived results

The technological issue addressed in this article has direct industrial importance in material forming applications. The introduction of the fluid dynamics numerical simulation (Figs. 3–10) provides us with a better understanding of physical simulation results in Figs. 1–2.

Addressing Eqs. (A1)–(A2) in Appendix A again, the partial derivatives of dimensionless flow function ψ define the flow velocity components: $\partial\psi/\partial y = u$; $\partial\psi/\partial x = (-v)$. In the 3-D spatial diagrams for flow function ψ in Fig. 4 near the die corner b with rectangular Cartesian coordinates $(0, -40)$ we have the following effect of punch shape ad-AD on dead zone dDb size. With the application of a rectangular punch with $2\theta_0 = 90^\circ$ in Figs. 1b, 3a, 4a, 5a, 6a, 7a, 8a, 9a, c, 10 we see a large dead zone dDb with zero flow function $\psi = 0$ (Fig. 4) and zero flow velocities $u = 0$ (Fig. 6); $v = 0$ (Fig. 7). But with the introduction of an inclined 2θ -

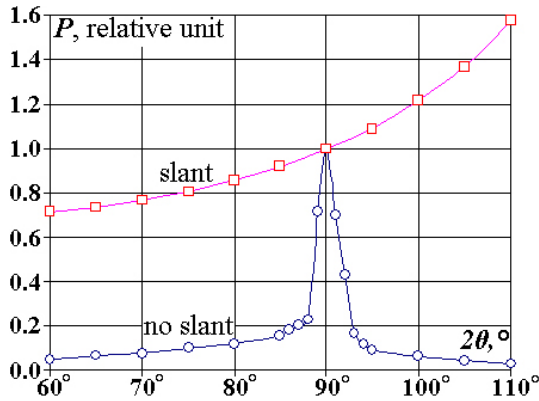


Figure 10. Computational dimensionless punching pressures for plasticine viscous liquid flow through Segal dies with $60^\circ \leq 2\theta \leq 110^\circ$ for the rectangular punch dD ($2\theta_0 = 90^\circ$) (○) and for the modified $2\theta_0$ -inclined or $2\theta_0$ -beveled punch dD ($2\theta_0 = 2\theta$) (□).

punch with $2\theta_0 = 75^\circ$ (inclined punch in Figs. 1a, c, 2, 3b, 4b, 5b, 6b, 7b, 8b, 9b, d, 10) we see a smaller dead zone size dDb. Computational flow lines (Fig. 3) are the lines near which flow function ψ (Fig. 4) is constant $\psi = \text{const}$. The computed effect in Fig. 4, which shows the absence of the “sawtooth” shape of the ψ -function over the die area dDb confirms that the dDb area is just the dead zone and not a vortex or eddy zone with circulating flow. Figure 5 show us that the curl function $\zeta = 0$ is also zero in the dead zone dDb.

Polycrystalline material is a natural composite, which contains ultra fine single crystals and amorphous viscous fluid between single crystals for fastening and connecting these single crystals among themselves. Laminar-flow layers of such amorphous fluid move with different velocities as well as single crystal sides, adjacent to laminar-flow layers. Curl ζ (Eq. A2) characterizes single crystal relative rotation during its linear displacement along the flow lines in Fig. 5. As a result of internal friction the contacting facets of single crystals become smooth like smoothing of river or sea pebbles under action of viscous flow.

This is the hydrodynamic explanation of the increase of the material plasticity during ECAP, which follows from the computational diagrams in Figs. 3–10. Under the action of mechanical loads at the boundaries of the contacting facets of single crystals, there appear no micro-cracks because of their flatness. The curl is zero in dead zone dDb. So in the material dead zone dDb no smoothing of single crystals facets takes place. As a result, material plasticity cannot be improved in the material dead zone dDb.

Such hydrodynamic illustrations (Figs. 3–10) directly confirm experimentally derived results (Figs. 1–2) with physical simulation of punch shape effect on material flow kinematics during ECAE through the acute-angled Segal 2θ -die.

6 Conclusions

In the present work we addressed the $2\theta_0$ -punch shape effect on material flow dynamics during ECAP through the numerical solution of the boundary value problem Eqs. (A1)–(A2), (B1), (C1)–(C7) for Navier–Stokes equations in curl transfer form (Figs. 3–10), taking into account the standard rectangular and improved $2\theta_0$ -inclined or $2\theta_0$ -beveled punch shapes.

Both physical (Fig. 1b) and fluid dynamics (Figs. 3a, 4a, 5a, 6a, 7a, 8a, 9a, c, 10) simulations show that the application of a standard rectangular punch with $2\theta_0 = 90^\circ$ for workpiece ECAP through acute-angled Segal 2θ -dies with $2\theta < 90^\circ$ is highly undesirable because of the resulting large material dead zone areas dDb in the neighborhood of the external die angle $2\theta = \angle(abc)$.

Both physical (Figs. 1a, c and 2) and fluid dynamics (Figs. 3b, 4b, 5b, 6b, 7b, 8b, 9b, d, 10) simulations reveal that the introduction of $2\theta_0$ -inclined or $2\theta_0$ -beveled punch shapes with dDbc for material ECAP processing through the acute-angled Segal 2θ -dies with $2\theta < 90^\circ$ and $2\theta_0 = 2\theta$ is a very promising technique because of minimal material dead zone areas dDb and the resulting minimal material waste in the neighborhood of external die angle $2\theta = \angle(abc)$, e.g. for $2\theta = 75^\circ$.

Appendix A: Navier–Stokes equations in curl transfer form

The curl transfer equation in dimensionless variables will have the following form (Roache, 1976):

$$\frac{\partial \zeta}{\partial t} = -Re \left(\frac{\partial(u\zeta)}{\partial x} + \frac{\partial(v\zeta)}{\partial y} \right) + \left(\frac{\partial^2 \zeta}{\partial x^2} + \frac{\partial^2 \zeta}{\partial y^2} \right), \quad (A1)$$

where the dimensionless curl function will be defined as (Fig. 5):

$$\zeta = \frac{\partial u}{\partial y} - \frac{\partial v}{\partial x}. \quad (A2)$$

Appendix B: Initial conditions for curl transfer equation

We now study the steady-state regime of viscous flow for a physical model of polymer material (Figs. 3–10). So the initial conditions we will assume in the form of a rough approximation to the stationary solution (Figs. 3–10):

$$u_{i,j}^0 = 0; \quad v_{i,j}^0 = 0; \quad \zeta_{i,j}^0 = 0; \quad \psi_{i,j}^0 = 0. \quad (B1)$$

Appendix C: Boundary conditions for curl transfer equation

The boundary conditions for the die walls we will define as the viscous material “sticking” to the walls of the die (Figs. 3–10).

At the inner upper boundary DBC (Figs. 3–10) we have

$$\psi_{i,j} = 1; \quad \zeta_{i,j} = 1. \quad (C1)$$

At the external lower boundary dbc (Figs. 3–10) we have

$$\psi_{i,j} = 0; \quad \zeta_{i,j} = 0. \quad (C2)$$

For the punch frontal edge dD (Figs. 3–10) we have

$$\psi_{10,-10} = 1; \quad \psi_{9,-11} = 1 - 2/N; \\ \psi_{i,j} = \psi_{i+2,j+2} - 2/N, \quad (C3)$$

where N is the quantity of ordinate steps along the channel width.

For the angular points, which are located in the vertices of the concave angles b and B (Figs. 3–10) we have

$$\zeta_{i,j} = 0. \quad (C4)$$

For the angular point D (Figs. 3–10) of the convex angle in the finite-difference equation, written for the mesh point (10, –11) we have the following curl

$$\zeta_{10,10} = 2\psi_{10,-11}. \quad (C5)$$

For the angular point D (Figs. 3–10) of the convex angle in the finite-difference equation, written for the mesh point (11, 10) we have the curl

$$\zeta_{10,10} = 2\psi_{11,10}. \quad (C6)$$

At the outlet line cC we have

$$\psi_{N+1,j} = \psi_{N-3,j} - 2\psi_{N-2,j} + 2\psi_{N,j}; \\ \zeta_{N+1,j} = \zeta_{N-3,j} - 2\zeta_{N-2,j} + 2\zeta_{N,j}. \quad (C7)$$

Appendix D: Numerical values of physical parameters for the problem

The numerical results of integration of curl transfer Eqs. (A1)–(A2) with initial Eq. (B1) and boundary Eqs. (C1)–(C7) conditions are outlined in Figs. 3–10 for the following numerical values:

- the dimensional width of inlet and outlet die channels is $\bar{a} = 35$ mm;
- the dimensional length of die channel is $\bar{L} = 16 \cdot \bar{a} = 16 \cdot 35 \times 10^{-3}$ m = 0.56 m;
- the dimensional average ECAP punching velocity is $\bar{U}_0 = 0.1 \times 10^{-3}$ m s^{–1};
- the dimensional time of processed workpiece material motion in die channel is $\bar{t}^* = \bar{L}/\bar{U}_0 = 0.56/(0.1 \times 10^{-3}) = 5600$ s;
- the maximum value of dimensionless curl is $\zeta = 1$;
- the dimensional curl is $\bar{\zeta} = \zeta \cdot \bar{U}_0/\bar{a} = (1 \times 0.1 \times 10^{-3} \text{ m s}^{-12})/(35 \times 10^{-3} \text{ m}) = 2.86 \times 10^{-3} \text{ s}^{-1}$;
- the dimensional average angular velocity of rotation for viscous material layers is $\bar{\omega} = |\text{rot}w|/2 = \bar{\zeta}/2 = 1.43 \times 10^{-3} \text{ s}^{-1}$;
- the number of turns for viscous material layers during the time of workpiece material motion in die channel is $N^* = \bar{\omega}\bar{t}^*/2\pi = (1.43 \times 10^{-3} \times 5600)/2 \times 3.14 = 1.27$;
- the dimensional density of the viscous plasticine physical model of extruded polymer material is $\bar{\rho} = 1850 \text{ kg m}^{-3}$;
- the dimensional plasticine yield strength is $\bar{\sigma}_s = 217 \text{ kPa}$ (Sofuoglu and Rasty, 2000);
- the dimensional specific heat capacity of plasticine material is $\bar{c} = 1.004 \text{ kJ}/(\text{kg K}^{-1})$;
- the dimensional thermal conductivity is $\bar{\lambda} = 0.7 \text{ J}/(\text{m s}^{-1} \text{ K}^{-1})$ (Chijiwa et al., 1981);
- the dimensional punching temperature is $\bar{t}_{\text{temp}} = 20$ °C;
- the dimensional dynamic viscosity for viscous Newtonian fluid model of plasticine workpiece during ECAE is $\bar{\eta}_{\text{vis}} = 1200 \text{ kPa s}^{-1}$;

- the dimensional kinematic viscosity for viscous Newtonian fluid model of plasticine workpiece during ECAE is $\bar{\nu}_{\text{vis}} = \bar{\eta}_{\text{vis}}/\bar{\rho} = 1.2 \times 10^6/1850 = 648.648 \text{ m}^2 \text{ s}^{-1}$;
- Reynolds number is $Re = \bar{U}_0 \bar{a} \bar{\rho} / \bar{\eta}_{\text{vis}} = \bar{U}_0 \bar{a} / \bar{\nu}_{\text{vis}} = 5.396 \times 10^{-9}$;
- the half number of coordinate steps along the x and y axes is $N = 40$;
- the number of coordinate steps along the x and y axes is $2 \times N = 80$;
- the relative error of iterations is $e = 1/1000$;
- the dimensional time moment for the first isochrone building is $t_1 = 100 \text{ s}$;
- die channel intersection angle of Segal die is $2\theta = 75^\circ$;
- punch shape inclination angles adD are $2\theta_0 = 90^\circ$ (rectangular punch in Figs. 1b, 3a, 4a, 5a, 6a, 7a, 8a, 9a, c, 10) and $2\theta_0 = 75^\circ$ (inclined punch in Figs. 1a, c, 3b, 4b, 5b, 6b, 7b, 8b, 9b, d, 10);
- the dimensional horizontal and vertical coordinate steps along the x - and y axes are $\bar{\xi} = 1.10 \text{ mm}$ and $\bar{\eta} = 1.44 \text{ mm}$ for angular die with $2\theta = 75^\circ$;
- the dimensional time iteration step is $\bar{\tau} = \bar{t}_{\text{it}} = 610 \mu\text{s}$ for ECAP die with $2\theta = 75^\circ$;
- the dimensional transition time is $\bar{t}_{\text{tr}} = 11.3 \text{ s}$ for ECAP die with $2\theta = 75^\circ$.

Acknowledgements. Authors thank three “anonymous” referees for their valuable notes and suggestions. Authors are thankful to Mechanical Sciences Editors and Copernicus GmbH Team for this great opportunity to publish our original research at your respectful periodical Mechanical Sciences under a Creative Commons License.

Edited by: A. Barari

Reviewed by: three anonymous referees

References

- Boulahia, R., Gloaguen, J.-M., Zairi, F., Naït-Abdelaziz, M., Seguela, R., Boukharouba, T., Lefebvre, J. M.: Deformation behaviour and mechanical properties of polypropylene processed by equal channel angular extrusion: Effects of back-pressure and extrusion velocity, *Polymer*, 50, 5508–5517, doi:10.1016/j.polymer.2009.09.050, 2009.
- Chijiwa, K., Hatamura, Y., and Hasegawa, N.: Characteristics of plasticine used in the simulation of slab in rolling and continuous casting, *T. Iron Steel I. Jpn.*, 21, 178–186, doi:10.2355/isijinternational1966.21.178, 1981.
- Haghighi, R. D., Jahromi, A. J., and Jahromi, B. E.: Simulation of aluminum powder in tube compaction using equal channel angular extrusion, *J. Mater. Eng. Perform.*, 21, 143–152, doi:10.1007/s11665-011-9896-1, 2012.
- Han, W. Z., Zhang, Z. F., Wu, S. D., and Li, S. X.: Investigation on the geometrical aspect of deformation during equal-channel angular pressing by in-situ physical modeling experiments, *Mat. Sci. Eng. A*, 476, 224–229, doi:10.1016/j.msea.2007.04.114, 2008.
- Laptev, A. M., Perig, A. V., and Vyal, O. Y.: Analysis of equal channel angular extrusion by upper bound method and rigid blocks model, *Mat. Res., São Carlos (Mater. Res.-Ibero-Am. J.)*, 17, 359–366, doi:10.1590/S1516-14392013005000187, 2014.
- Minakowski, P.: Fluid model of crystal plasticity: numerical simulations of 2-turn equal channel angular extrusion, *Tech. Mechanik*, 34, 213–221, 2014.
- Nagasekhar, A. V., Tick-Hon, Y., and Ramakanth, K. S.: Mechanics of single pass equal channel angular extrusion of powder in tubes, *Appl. Phys. A*, 85, 185–194, doi:10.1007/s00339-006-3677-y, 2006.
- Nejadseyfi, O., Shokuhfar, A., Azimi, A., and Shamsborhan, M.: Improving homogeneity of ultrafine-grained/nanostructured materials produced by ECAP using a bevel-edge punch, *J. Mater. Sci.*, 50, 1513–1522, doi:10.1007/s10853-014-8712-3, 2015.
- Perig, A. V.: 2D upper bound analysis of ECAE through 2θ -dies for a range of channel angles, *Mat. Res., São Carlos (Mater. Res.-Ibero-Am. J.)*, 17, 1226–1237, doi:10.1590/1516-1439.268114, 2014.
- Perig, A. V. and Laptev, A. M.: Study of ECAE mechanics by upper bound rigid block model with two degrees of freedom, *J. Braz. Soc. Mech. Sci. Eng.*, 36, 469–476, doi:10.1007/s40430-013-0121-z, 2014.
- Perig, A. V. and Golodenko, N. N.: CFD Simulation of ECAE through a multiple-angle die with a movable inlet wall, *Chem. Eng. Commun.*, 201, 1221–1239, doi:10.1080/00986445.2014.894509, 2014a.
- Perig, A. V. and Golodenko, N. N.: CFD 2D simulation of viscous flow during ECAE through a rectangular die with parallel slants, *Int. J. Adv. Manuf. Technol.*, 74, 943–962, doi:10.1007/s00170-014-5827-2, 2014b.
- Perig, A. V., Laptev, A. M., Golodenko, N. N., Erfort, Y. A., and Bondarenko, E. A.: Equal channel angular extrusion of soft solids, *Mat. Sci. Eng. A*, 527, 3769–3776, doi:10.1016/j.msea.2010.03.043, 2010.
- Perig, A. V., Zhibankov, I. G., and Palamarchuk, V. A.: Effect of die radii on material waste during equal channel angular extrusion, *Mater. Manuf. Process.*, 28, 910–915, doi:10.1080/10426914.2013.792420, 2013a.
- Perig, A. V., Zhibankov, I. G., Matveyev, I. A., and Palamarchuk, V. A.: Shape effect of angular die external wall on strain unevenness during equal channel angular extrusion, *Mater. Manuf. Process.*, 28, 916–922, doi:10.1080/10426914.2013.792417, 2013b.
- Perig, A. V., Tarasov, A. F., Zhibankov, I. G., and Romanko, S. N.: Effect of 2θ -punch shape on material waste during ECAE through a 2θ -die, *Mater. Manuf. Process.*, 30, 222–231, doi:10.1080/10426914.2013.832299, 2015.
- Rejaeian, M. and Aghaie-Khafri, M.: Study of ECAP based on stream function, *Mech. Mater.*, 76, 27–34, doi:10.1016/j.mechmat.2014.05.004, 2014.
- Roache, P. J.: *Computational fluid dynamics*, Hermosa Publishers, Albuquerque, 1976.
- Segal, V. M.: Engineering and commercialization of equal channel angular extrusion (ECAE), *Mat. Sci. Eng. A*, 386, 269–276, doi:10.1016/j.msea.2004.07.023, 2004.
- Sofuoğlu, H. and Rasty, J.: Flow behavior of Plasticine used in physical modeling of metal forming processes, *Tribol. Int.*, 33, 523–529, doi:10.1016/S0301-679X(00)00092-X, 2000.
- Wu, Y. and Baker, I.: An experimental study of equal channel angular extrusion, *Scripta Mater.*, 37, 437–442, doi:10.1016/S1359-6462(97)00132-2, 1997.